Review Article | Genitourinary Imaging

https://doi.org/10.3348/kjr.2017.18.4.597
pISSN 1229-6929 · eISSN 2005-8330
Korean J Radiol 2017;18(4):597-606

Korean Journal of Radiology
KJR

Multiparametric MRI in the Detection of Clinically Significant Prostate Cancer

Jurgen J. Fütterer, MD, PhD

Department of Radiology and Nuclear Medicine, Radboud University Medical Center, Nijmegen 6500HB, the Netherlands

Prostate cancer is the most common cancer among men aged 50 years and older in developed countries and the third leading cause of cancer-related death in men. Multiparametric prostate MR imaging is currently the most accurate imaging modality to detect, localize, and stage prostate cancer. The role of multi-parametric MR imaging in the detection of clinically significant prostate cancer are discussed. In addition, insights are provided in imaging techniques, protocol, and interpretation.
Keywords: *MRI prostate cancer; Magnetic resonance imaging; Multiparametric MRI; Prostate; PI-RADS*

INTRODUCTION

Prostate cancer is the most common cancer among men aged 50 years and older in developed countries and the third leading cause of cancer-related death in men (1). With the widespread use of prostate-specific antigen (PSA) screening and increasing life expectancy, more men are being diagnosed with localized, low-risk, low-grade prostate cancer (2). However, the PSA test lacks specificity in the detection of prostate cancer (3). Diagnosis is a challenge in cases with elevated or increasing PSA level and negative findings on the subsequent transrectal ultrasound-guided 12-core biopsy. Over 20% of the prostate cancers are missed or undersampled during the first biopsy session (4). Moreover, prostatitis or benign prostatic hyperplasia (BPH) also cause elevated or increased PSA levels. This diagnostic uncertainty is a common concern in daily practice, which often results in additional biopsy sessions with varying success rates (range 10–40%) (4-7).

Multiparametric prostate MR imaging (mpMRI) is currently the most accurate imaging modality to detect, localize, and stage prostate cancer (8). Prostate MR imaging can provide both functional tissue information and anatomical information. To increase the diagnostic accuracy, anatomical T2-weighted MR imaging and functional MR imaging techniques such as dynamic contrast-enhanced MR imaging (DCE-MRI) and diffusion-weighted imaging (DWI) should be combined in an integrated mpMRI prostate examination. Each of the techniques have unique strengths and shortcomings, however, the combination may overcome these shortcomings (9).

Multiparametric prostate MR imaging of the prostate detects both high grade and larger tumors accurately. Thus, it may perform particularly well for the detection of clinically significant disease. Evidence is being gathered to identify cancers of significant volume. Moreover, these functional techniques may be used to differentiate between low- and intermediate/high-grade prostate cancer (10-12). Due to these characteristics, mpMRI is a potential tool to rule out significant disease. DWI is the most promising

Received November 17, 2016; accepted after revision February 20, 2017.
Corresponding author: Jurgen J. Fütterer, MD, PhD, Department of Radiology and Nuclear Medicine, Radboud University Medical Center, Geert grooteplein 10, Nijmegen 6500HB, the Netherlands.
• Tel: (3124) 361 4011 • Fax: (3124) 354 0866
• E-mail: jurgen.futterer@Radboudumc.nl

technique to investigate not only the size but also the aggressiveness of the respective tumor.

At present, prostate mpMRI reporting is becoming increasingly standardized by using the Prostate Imaging Reporting And Data System (PI-RADS). In this study, we discuss the recently introduced second version of this classification (13). In addition, the role of mpMRI in the detection of clinical significant prostate cancer is discussed. Insights are provided in imaging techniques, protocol, and interpretation.

MR Imaging Techniques

T2-Weighted MR Imaging

T2-weighted MR imaging has the highest in-plane spatial resolution compared to the other imaging sequences included in the prostate mpMRI (i.e., DWI and DCE-MRI) and is crucial in the assessment of capsular and neurovascular bundle involvement. Due to the high spatial resolution and soft tissue contrast, T2-weighted imaging is ideal to differentiate between the high-signal-intense peripheral zone and the low-signal-intense central and heterogeneous transition zone. In aging men, BPH commonly compresses the central zone, which leads to difficulty in recognizing the remaining central zone on T2-weighted MR imaging. The central gland mostly comprises a transition zone in aging men, such that the prostate is roughly divided into a peripheral zone and a transition zone radiologically (14).

The high-signal intensity of the peripheral zone may be disrupted due to the presence of prostate cancer.

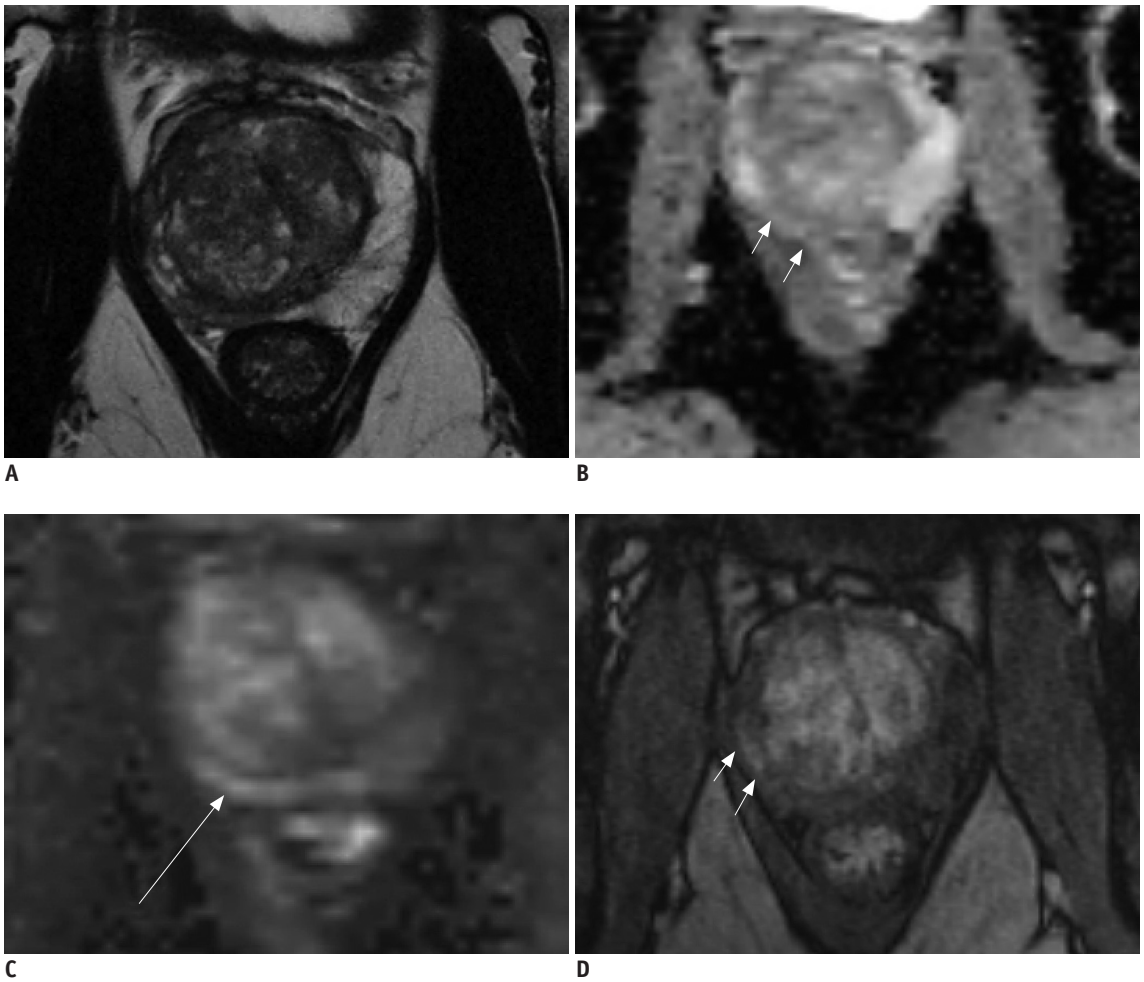

Fig. 1. 61-year-old male with fluctuating PSA and current PSA level of 7.5 ng/mL. Prior biopsy session revealed no prostate cancer. **A.** T2-weighted MR imaging demonstrates asymmetric right peripheral zone with volume loss. Low signal intensity can be observed in right peripheral zone. **B, C.** ADC map **(B)** demonstrates intermediate signal intensity in right peripheral zone (arrows) and high b-value image **(C)** demonstrate intermediate to high signal intensity (arrow). **D.** T1-weighted post-contrast image demonstrates early uptake of contrast material in right peripheral zone (arrows). MR image guided biopsy revealed prostatitis and fibrosis. ADC = apparent diffusion coefficient, PSA = prostate-specific antigen

Korean Journal of Radiology
KJR

However, benign conditions like fibrosis, hemorrhage, atrophy, and prostatitis (Fig. 1) frequently lower the signal intensity in the peripheral zone and thus mimic prostate cancer. Commonly, a differentiation can be made based on morphologic features. A focal, round, or irregular structure is more likely to be prostate cancer; whereas, prostatitis, for example, is marked by a wedge-shaped and diffuse morphology.

The transition zone is characterized by heterogeneous signal intensities. In the transition zone, BPH may obscure or mimic prostate cancer. BPH mostly appears as nodules with circumscribed margins (low signal intensity) (Fig. 2). Routinely, BPH nodules are characterized by the mixture of hyper- and hypo-signal-intensity (15). Based on these characteristics, often a distinction can be made between a benign nodule and prostate cancer. Features indicative of transition zone cancers include homogenous low T2 signal intensity, ill defined margins, lack of capsule, lenticular shape, and invasion of anterior fibromuscular stroma (16). The presence of an "erased charcoal sign" in a lenticular lesion is highly suggestive of cancer (9). To increase the diagnostic accuracy of MRI for prostate cancer, T2-weighted images should be used in conjunction with functional imaging techniques.

Diffusion-Weighted Imaging

DCE-MRI is based upon measuring the Brownian motion of water molecules within a voxel of tissue. Free water molecules are in constant random motion, known as Brownian motion, which is related to thermal kinetic energy. In the prostate, the most common method used for DWI is to incorporate two symmetric motion-probing gradient pulses into a single-shot spin-echo T2-weighted sequence.

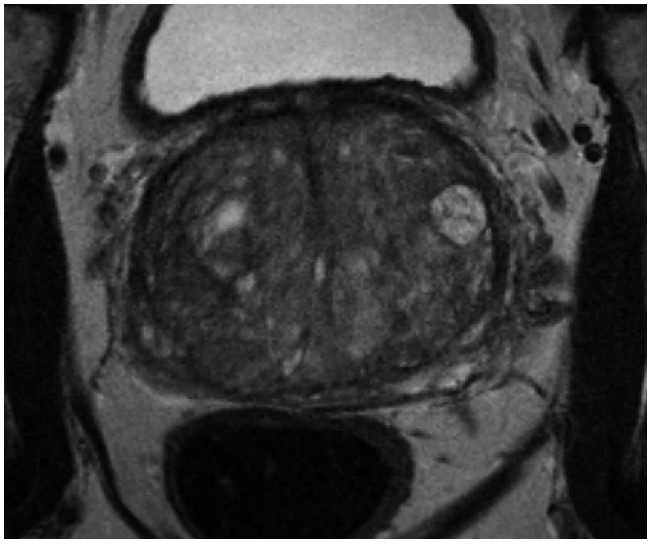

Fig. 2. 75-year-old male with PSA level of 21 ng/mL. T2-weighted MR imaging reveals multiple BPH nodules (organized chaos) in transition zone. BPH = benign prostatic hyperplasia, PSA = prostate-specific antigen

DWI consists of two components: a b-value and an apparent diffusion coefficient (ADC). The b-value reflects the strength of the diffusion sensitizing gradient. The b-value is measured in seconds per square millimeter and thus reflects the amount of diffusion weighting. In prostate DWI, different sensitizing gradients (b-values) are used for optimal evaluation of aberrant lesions in the prostate. Small b-values only result in signal loss of highly mobile water molecules (like blood in a vessel). Like other cancers, prostate cancer tends to have higher cellular density and an excess of intra- and intercellular membranes compared with normal glandular tissue (17). High cellular tissue occurs in other conditions besides prostate cancer; among these, BPH, prostatitis and fibrosis are examples of benign tissue, which may be marked by a high signal on b-value imaging and a low signal on the ADC map as well. These benign conditions often hamper the DWI assessment of prostate cancer, as in T2-weighted imaging. Further, DWI is very susceptible to artifacts (i.e., motion or bowel movement and susceptibility).

Dynamic Contrast-Enhanced MR Imaging

Dynamic contrast-enhanced MR imaging represents the vascular properties of tissue. The microvascular network formed by the capillaries supplies the tissues and facilitates their function. The ability of the tumor to generate new blood vessels is a critical influencing factor for its development, growth, invasiveness, and progression into the metastatic form. Angiogenesis, the sprouting of new capillaries from existing blood vessels, and vasculogenesis, the *de novo* generation of new blood vessels, are the two primary methods of vascular expansion by which nutrient supply to tumor tissue is adjusted to match physiologic needs (18). The importance of angiogenesis in prostate cancer is well established. Dynamic susceptibility MR sequences (T2*-weighted) are sensitive to the vascular phase of contrast medium delivery, which reflect the tissue perfusion and blood volume. However, there is limited evidence for its clinical application in the prostate.

DCE-MRI consists of a series of fast T1-weighted sequences covering the entire prostate before and after

rapid injection of a bolus of a low-molecular-weight gadolinium chelate. DCE-MRI following the administration of low molecular weight contrast media (< 1 kDa) is the most common imaging method for evaluating human tumor vascular function *in situ* (19). Assessment of signal intensity changes on T1-weighted DCE-MRI to estimate the contrast agent uptake *in vivo* can be performed qualitatively, semiquantitatively, or quantitatively. The qualitative analysis of signal intensity changes can be achieved by assessing the shape of the signal intensity-time curve. Furthermore, the location of early enhancement is correlated with the finding(s) from the T2-weighted MR sequence or DWI.

Like other cancerous tissue, prostate cancer is highly vascularized. The hemodynamic properties of prostate cancer are characterized by an early and intense enhancement and subsequently a rapid wash-out. However, the assessment of DCE-MRI in the peripheral zone is hampered by highly vascularized prostatitis. Within the transition zone, the appreciation of DCE-MR is difficult due to sometimes highly perfused BPH nodules.

MRI Detection of Clinically Significant Disease

Gleason Grade Assessment

The Gleason grading system remains one of the most effective prognostic factors in prostate cancer (20). Gleason score, PSA level, and clinical stage have major roles in developing a treatment strategy. They have been associated with biochemical failure, local recurrences, and distant metastases such as skeletal and lymph node metastasis after prostatectomy or radiation therapy (21, 22). At present, there is no universally accepted definition of clinically significant disease, either at prostate biopsy or at definitive pathology after radical prostatectomy (23). mpMRI detects both high grade and larger tumours accurately and may thus perform particularly well for the detection of clinically significant disease (8). The recommended requirements of each pulse sequence are provided in Table 1.

Prostate mpMRI has demonstrated a good accuracy for differentiating between Gleason score ≤ 3 + 4 vs. Gleason score ≥ 4 + 3 in tumor volumes ≥ 0.5 mL (Figs. 3, 4) (23). Gleason scores of 3 + 4 and 3 + 3 are associated with lower disease progression rates, and Gleason scores of ≥ 4 + 3 are associated with higher disease progression rates (24). To differentiate between these two groups, mpMRI has shown value for discriminating tumors with varying degrees of aggressiveness using metrics derived from DWI (10, 25-27), DCE-MRI (28), and MR spectroscopic imaging (11). Several studies reported on the correlation of Gleason score with MR imaging using DWI. A negative correlation between Gleason grade and ADC values is reported (27, 29), with more significant correlation, as the prostate cancer is less differentiated ($p < 0.001$), with Gleason score of ≥ 7 (30). Although DWI shows differences between prostatitis (Fig. 5) and prostate cancer in both the peripheral zone and central gland, its usability in clinical practice is limited as a result

Table 1. Recommended Requirements for Each Sequence in mpMRI of Prostate (9, 49)

Sequence	Orientation	FOV (cm)	In-Plane Resolution (mm)	Slice-Thickness (mm)*	Gap (%)	TE (msec)	TR (msec)	b-values
T2-weighted (RARE/FSE/TSE)	Axial (2D)	12–20	≤ 0.7 (phase) ≤ 0.4 (frequency)	≤ 4	0			
	Coronal (2D)	12–20	≤ 0.7 (phase) ≤ 0.4 (frequency)	≤ 4	0			
	Sagittal (2D)	12–20	≤ 0.7 (phase) ≤ 0.4 (frequency)	≤ 4	0			
T1-weighted	Axial (2D)	12–20	≤ 1 (phase and frequency)	≤ 4	0	< 5 msec	< 100 msec	
DWI	Axial (2D)	16–22	≤ 2.5 (phase and frequency)	≤ 4	0	≤ 90	≥ 3000	50–100 and 800–1000
DWI (high b-value)†	Axial (2D)	16–22	≤ 2.5 (phase and frequency)	≤ 4	0	≤ 90	≥ 3000	≥ 1400
DCE-MRI‡	Axial (2D or 3D)	12–20	≤ 2.0 (phase and frequency)	≤ 4	0	< 5 msec	< 100 msec	

*Locations should be same as those used for T2-weighted, DWI and DCE-MRI, †Either acquired or extrapolated high b-value images, ‡Temporal resolution: ≤ 10 sec (< 7 sec is preferred) with total observation rate of > 2 min. DCE-MRI = dynamic contrast-enhanced MR imaging, DWI = diffusion-weighted imaging, FOV = field of view, FSE = fast spin echo, mpMRI = multiparametric prostate MR imaging, MR = magnetic resonance, RARE = rapid acquisition with relaxation enhancement, TE = echo time, TR = relaxation time, TSE = turbo spin echo

Korean Journal of Radiology
KJR

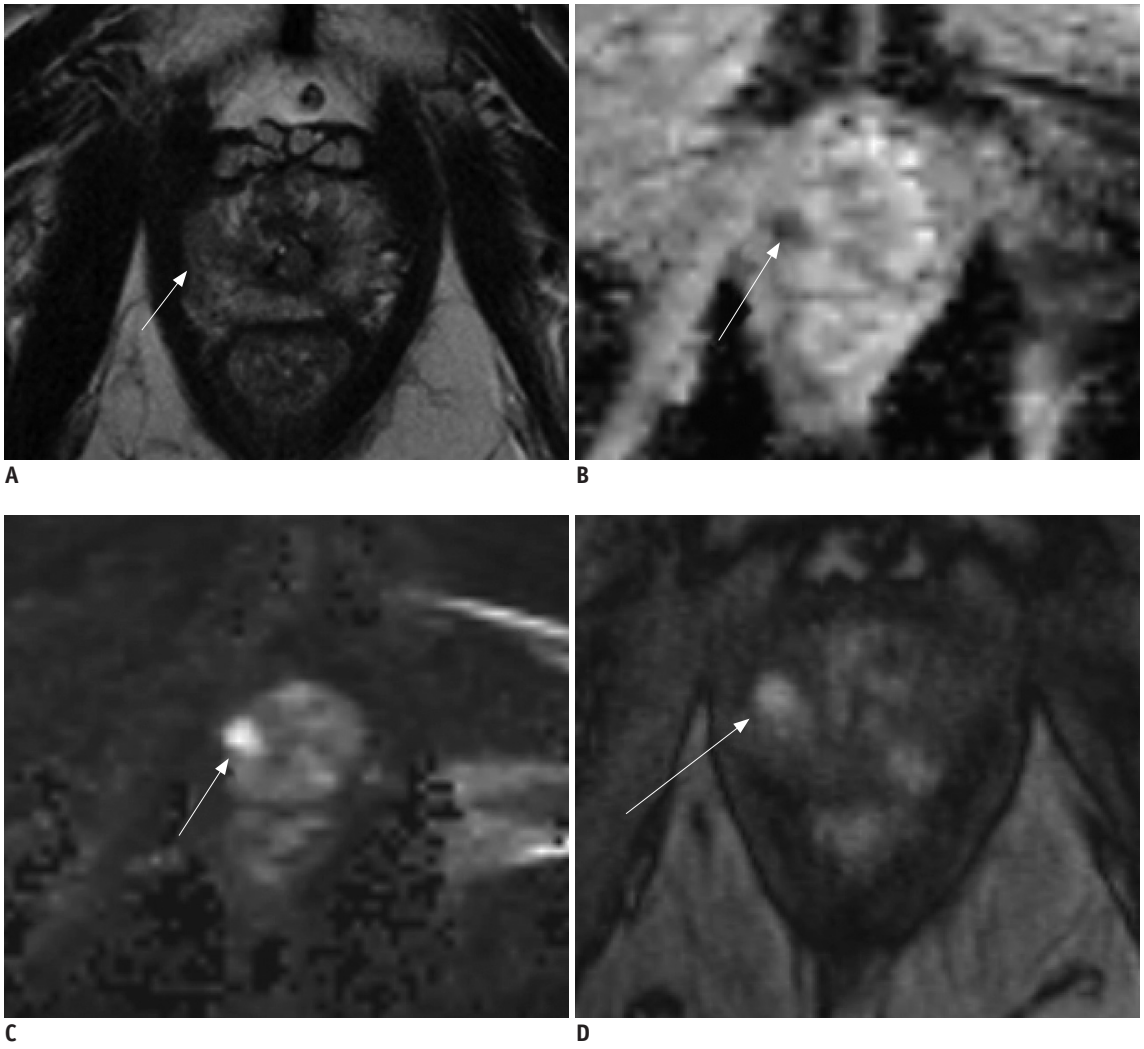

Fig. 3. 62-year-old male with PSA level of 5.6 ng/mL.
A. T2-weighted MR imaging reveals low signal intensity lesion (arrow) in right apex. **B, C.** ADC map **(B)** demonstrates distinct low signal intensity in right peripheral zone (arrow) and high b-value image **(C)** demonstrates high signal intensity (arrow). **D.** T1-weighted post-contrast image demonstrates early uptake of contrast material at corresponding location (arrow) **(A-C)**. MR image targeted biopsy revealed Gleason 4 + 3 prostate cancer. ADC = apparent diffusion coefficient, PSA = prostate-specific antigen

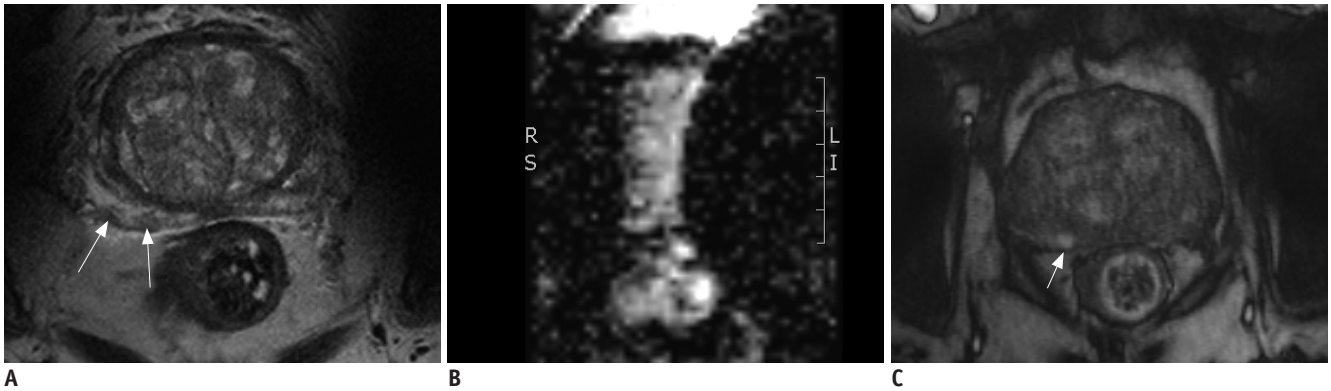

Fig. 4. 78-year-old male with PSA level of 10.2 ng/mL and two negative prior transrectal ultrasound-guided biopsy sessions.
A. T2-weighted MR imaging reveals low signal intensity lesion (arrows) in right peripheral zone. **B.** ADC map is not diagnostic as result of bilateral hip implants. **C.** T1-weighted post-contrast image demonstrates early uptake of contrast material at corresponding location (arrow) **(A)**. MR image targeted biopsy revealed Gleason 3 + 4 prostate cancer. ADC = apparent diffusion coefficient, PSA = prostate-specific antigen

of significant overlap in ADCs (31).

The choline plus creatine-to-citrate ratios acquired by using MR spectroscopic imaging demonstrated a correlation with Gleason grade in cancer foci located in the peripheral zone (32). Only limited information is available on the possible correlation of signal intensities measured on T2-weighted MR imaging with Gleason score (33). Currently, almost all studies have investigated the peripheral zone, mainly because 70–75% of the tumors are located in the peripheral zone and the transition zone remains a difficult area in which to assess tumor aggressiveness.

ADC parameters from whole-lesion histogram analysis can be used. The 10th percentile ADC correlates better with the Gleason score and more accurately differentiates lesions with a Gleason score of 6 from those with a Gleason score of ≥ 7 compared with other ADC parameters commonly used in the literature (10).

Tumor Volume Assessment with MRI

Thus far, few studies have focused on tumor volume estimation (34-36). In 2002, the value of MR spectroscopic imaging in measuring tumor volume in nodules > 0.5 cm^3 was assessed and researchers showed that it was positively correlated with histopathologic tumor volume with a Pearson correlation coefficient of 0.59 (37). More recently, studies on DCE-MRI and DWI have shown some promising results; however, there is a tendency to underestimate the actual tumor volume on histopathology of whole mount sections.

Tumor volume is underestimated by DWI especially for Gleason scores (≥ 7) and lesions with high suspicion score of 4/5 (38). T2-weighted MR imaging showed less underestimation of the actual tumor volume. Thus, a much

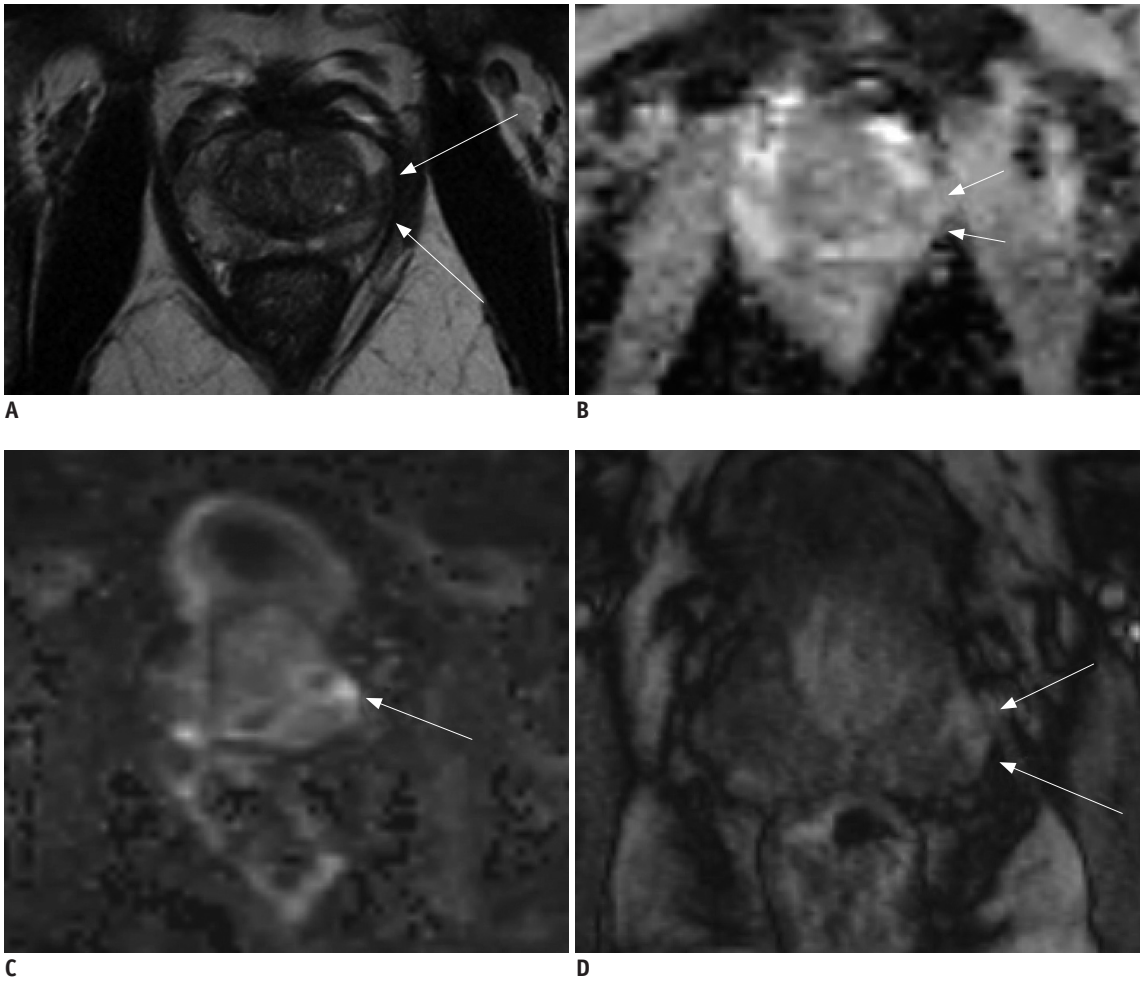

Fig. 5. 68-year-old male with PSA level of 2.5 ng/mL.
A. T2-weighted MR imaging reveals low signal intensity lesion (arrows) in left peripheral zone. **B, C.** ADC map **(B)** demonstrates distinct low signal intensity (arrows) and high b-value image **(C)** demonstrates high signal intensity at corresponding location (arrow) **(A)**. **D.** T1-weighted post-contrast image demonstrates early uptake of contrast material (arrows) at corresponding location **(A-C)**. MR image targeted biopsy revealed chronic prostatitis. ADC = apparent diffusion coefficient, PSA = prostate-specific antigen

Korean Journal of Radiology
KJR

larger region of the gland that is directly visualized on MRI warrants ablation to ensure full tumor destruction. This discrepancy in boundary may be most significant at the non-capsular side of the lesion, due to the tendency for tumors to originate close to the capsule and exhibit centripetal growth within the gland (39). These findings have key implications in planning and performing focal therapy procedures and would suggest the need for a security margin to ensure full tumor destruction in view of the larger histologic volume (40).

Tumor Stage Assessment with MRI

Clinical staging of prostate cancer currently entails the use of digital rectal examination, PSA measurement, as well as transrectal ultrasound. The clinical stage is identified using these variables and is expressed in the TNM staging classification. mpMRI is currently the most accurate imaging modality to pre-operatively stage prostate cancer (41). In local staging, T2-weighted MR imaging is the most important sequence. T2-weighted MR imaging has the highest in-plane spatial resolution compared to the other imaging sequences included in prostate MR imaging. Therefore, it is crucial in assessment of capsular and neurovascular bundle involvement. Despite the limited reports on the added value of DCE-MR imaging to improve staging performance, it does appear to improve local

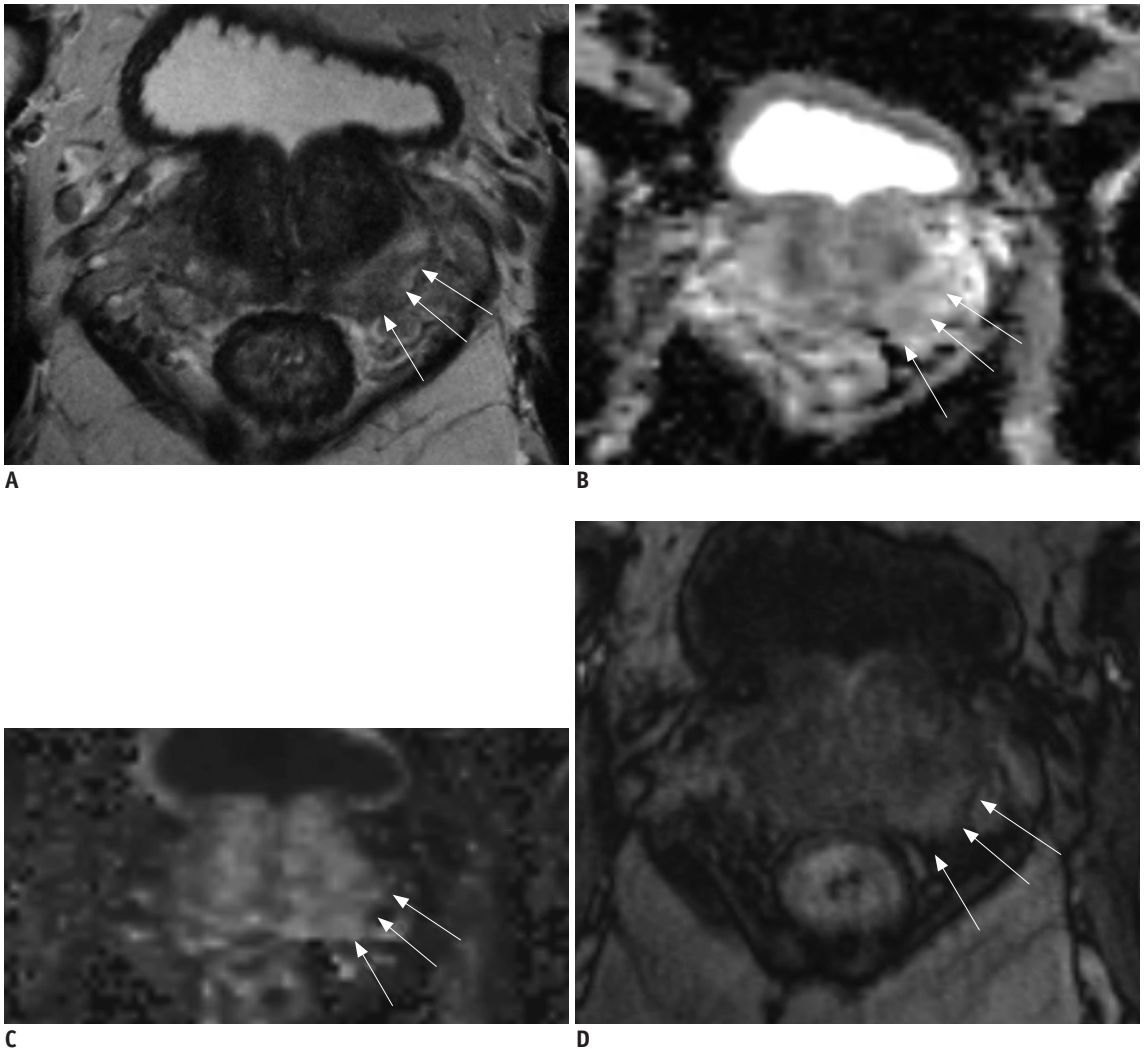

Fig. 6. 64-year-old male with PSA level of 4.9 ng/mL.
A. T2-weighted MR imaging reveals mild low signal intensity area (arrows) in left peripheral zone at base of prostate. **B, C.** ADC map **(B)** demonstrates mild low signal intensity (arrows) and high b-value image **(C)** demonstrates no high signal intensity at corresponding location (arrows) **(A)**. **D.** T1-weighted post-contrast image demonstrates early uptake of contrast material (arrows) at corresponding location **(A-C)**. Final PI-RADS assessment was 2. Clinical suspicion persisted and patient underwent MR image targeted biopsy which revealed Gleason 4 + 3 prostate cancer. ADC = apparent diffusion coefficient, PI-RADS = Prostate Imaging Reporting And Data System, PSA = prostate-specific antigen

staging performance when used in combination with T2-weighted imaging in patients with equivocal capsular penetration, seminal vesicle invasion, and neurovascular bundle involvement (42).

PI-RADS refers to a structured reporting scheme for evaluating the prostate for significant prostate cancer. PI-RADS version 2 (v2) was developed to further improve the accuracy and inter-observer agreement of the first version, as that version was limited by variable interpretations (9). PI-RADS v2 was developed by members of a Steering Committee using the best available evidence and expert consensus opinion (13). In addition, the use of a dominant sequence was introduced, which depends on the lesion location (peripheral zone or transition zone) and the employment of an overall score estimated from the individual scores of the used sequences.

In the appraisal of a lesion, first, the location of the lesion has to be defined. This determines the dominant sequence of the overall PI-RADS score (peripheral zone vs. transition zone). Mainly, the overall PI-RADS score of a lesion located in the peripheral zone follows the score of that lesion as determined with DWI. Only in case of an equivocal finding (PI-RADS 3), a positive score on DCE-MRI can upgrade the PI-RADS score to a 4. T2-weighted imaging plays a minor role in lesions located in the peripheral zone. T2-weighted imaging is the dominant sequence for lesions located in the transition zone. In this zone, DWI can upgrade the overall PI-RADS score in case of an equivocal finding on T2-weighted imaging: a PI-RADS 5 on DWI may upgrade a PI-RADS 3 lesion to PI-RADS score of 4.

Vargas et al. (43) reported that PI-RADS v2 correctly identified 94–95% of prostate cancer foci ≥ 0.5 mL, but was limited for the assessment of Gleason score ≥ 4 + 3 tumors ≤ 0.5 mL. Nevertheless, 5–6% of the significant cancers are missed with mpMRI (Fig. 6). Furthermore, PI-RADS v2 category 5 lesions are associated with higher Gleason scores and extraprostatic extension (44). Experienced radiologists reportedly achieve moderate reproducibility for PI-RADS v2, and neither require nor benefit from a training session (45). Increasing amounts of data are being published on the implications of PI-RADS v2. However, large multi-center studies are still lacking for both mpMRI and PI-RADS evaluation.

CONCLUSION

Prostate mpMRI is able to detect clinically significant disease. The detection rate of clinically significant disease ranges from 44 to 87%, which is higher compared to the reported findings of 'blind' transrectal ultrasound biopsy (23). In addition, mpMRI of the prostate is the standard imaging modality for tumor detection, localization, staging, treatment planning, and evaluation (46). Meta-analyses on prostate cancer detection by mpMRI revealed a specificity of 0.88 and sensitivity of 0.74 (95% confidence interval, 0.66–0.81) (47). DWI is the most promising sequence for assessing tumor aggressiveness. Nevertheless, there is still considerable overlap in ADC values between low- and intermediate/high risk prostate cancer lesions. Most likely, the signal-to-noise ratio is currently the major limitation. As a result, the highest in-plane resolution achievable with commercially available sequences, is in the range of 1.0–2.0 mm (9). Recently, high-resolution DWI of the prostate was introduced, which has the potential to further improve lesion characterization and visibility (48).

REFERENCES

1. Ferlay J, Shin HR, Bray F, Forman D, Mathers C, Parkin DM. Estimates of worldwide burden of cancer in 2008: GLOBOCAN 2008. *Int J Cancer* 2010;127:2893-2917
2. Stamey TA, Caldwell M, McNeal JE, Nolley R, Hemenez M, Downs J. The prostate specific antigen era in the United States is over for prostate cancer: what happened in the last 20 years? *J Urol* 2004;172(4 Pt 1):1297-1301
3. Thompson IM, Pauler DK, Goodman PJ, Tangen CM, Lucia MS, Parnes HL, et al. Prevalence of prostate cancer among men with a prostate-specific antigen level < or =4.0 ng per milliliter. *N Engl J Med* 2004;350:2239-2246
4. Djavan B, Ravery V, Zlotta A, Dobronski P, Dobrovits M, Fakhari M, et al. Prospective evaluation of prostate cancer detected on biopsies 1, 2, 3 and 4: when should we stop? *J Urol* 2001;166:1679-1683
5. Wang Y, Wang X, Yu J, Ouyang J, Shen W, Zhou Y, et al. Application of transrectal ultrasound-guided repeat needle biopsy in the diagnosis of prostate cancer in Chinese population: a retrospective study. *J Res Med Sci* 2016;21:79
6. Miyagawa T, Ishikawa S, Kimura T, Suetomi T, Tsutsumi M, Irie T, et al. Real-time virtual sonography for navigation during targeted prostate biopsy using magnetic resonance imaging data. *Int J Urol* 2010;17:855-860
7. Arsov C, Rabenalt R, Blondin D, Quentin M, Hiester A, Godehardt E, et al. Prospective randomized trial comparing magnetic resonance imaging (MRI)-guided in-bore biopsy to MRI-ultrasound fusion and transrectal ultrasound-guided prostate biopsy in patients with prior negative biopsies. *Eur Urol* 2015;68:713-720
8. Hoeks CM, Barentsz JO, Hambrock T, Yakar D, Somford DM,

Heijmink SW, et al. Prostate cancer: multiparametric MR imaging for detection, localization, and staging. *Radiology* 2011;261:46-66
9. Barentsz JO, Richenberg J, Clements R, Choyke P, Verma S, Villeirs G, et al. ESUR prostate MR guidelines 2012. *Eur Radiol* 2012;22:746-757
10. Donati OF, Mazaheri Y, Afaq A, Vargas HA, Zheng J, Moskowitz CS, et al. Prostate cancer aggressiveness: assessment with whole-lesion histogram analysis of the apparent diffusion coefficient. *Radiology* 2014;271:143-152
11. Kobus T, Hambrock T, Hulsbergen-van de Kaa CA, Wright AJ, Barentsz JO, Heerschap A, et al. In vivo assessment of prostate cancer aggressiveness using magnetic resonance spectroscopic imaging at 3 T with an endorectal coil. *Eur Urol* 2011;60:1074-1080
12. Peng Y, Jiang Y, Yang C, Brown JB, Antic T, Sethi I, et al. Quantitative analysis of multiparametric prostate MR images: differentiation between prostate cancer and normal tissue and correlation with Gleason score--a computer-aided diagnosis development study. *Radiology* 2013;267:787-796
13. Weinreb JC, Barentsz JO, Choyke PL, Cornud F, Haider MA, Macura KJ, et al. PI-RADS prostate imaging-reporting and data system: 2015, version 2. *Eur Urol* 2016;69:16-40
14. Vargas HA, Akin O, Franiel T, Goldman DA, Udo K, Touijer KA, et al. Normal central zone of the prostate and central zone involvement by prostate cancer: clinical and MR imaging implications. *Radiology* 2012;262:894-902
15. Ling D, Lee JK, Heiken JP, Balfe DM, Glazer HS, McClennan BL. Prostatic carcinoma and benign prostatic hyperplasia: inability of MR imaging to distinguish between the two diseases. *Radiology* 1986;158:103-107
16. Akin O, Sala E, Moskowitz CS, Kuroiwa K, Ishill NM, Pucar D, et al. Transition zone prostate cancers: features, detection, localization, and staging at endorectal MR imaging. *Radiology* 2006;239:784-792
17. desouza NM, Reinsberg SA, Scurr ED, Brewster JM, Payne GS. Magnetic resonance imaging in prostate cancer: the value of apparent diffusion coefficients for identifying malignant nodules. *Br J Radiol* 2007;80:90-95
18. Padhani AR, Harvey CJ, Cosgrove DO. Angiogenesis imaging in the management of prostate cancer. *Nat Clin Pract Urol* 2005;2:596-607
19. Collins DJ, Padhani AR. Dynamic magnetic resonance imaging of tumor perfusion. Approaches and biomedical challenges. *IEEE Eng Med Biol Mag* 2004;23:65-83
20. Epstein JI. Update on the Gleason grading system. *Ann Pathol* 2011;31(5 Suppl):S20-S26
21. Babaian RJ, Troncoso P, Bhadkamkar VA, Johnston DA. Analysis of clinicopathologic factors predicting outcome after radical prostatectomy. *Cancer* 2001;91:1414-1422
22. Zelefsky MJ, Kattan MW, Fearn P, Fearon BL, Stasi JP, Shippy AM, et al. Pretreatment nomogram predicting ten-year biochemical outcome of three-dimensional conformal radiotherapy and intensity-modulated radiotherapy for prostate cancer. *Urology* 2007;70:283-287
23. Fütterer JJ, Briganti A, De Visschere P, Emberton M, Giannarini G, Kirkham A, et al. Can clinically significant prostate cancer be detected with multiparametric magnetic resonance imaging? A systematic review of the literature. *Eur Urol* 2015;68:1045-1053
24. Chan TY, Partin AW, Walsh PC, Epstein JI. Prognostic significance of Gleason score 3+4 versus Gleason score 4+3 tumor at radical prostatectomy. *Urology* 2000;56:823-827
25. Vargas HA, Akin O, Franiel T, Mazaheri Y, Zheng J, Moskowitz C, et al. Diffusion-weighted endorectal MR imaging at 3 T for prostate cancer: tumor detection and assessment of aggressiveness. *Radiology* 2011;259:775-784
26. Rosenkrantz AB, Sigmund EE, Johnson G, Babb JS, Mussi TC, Melamed J, et al. Prostate cancer: feasibility and preliminary experience of a diffusional kurtosis model for detection and assessment of aggressiveness of peripheral zone cancer. *Radiology* 2012;264:126-135
27. Hambrock T, Somford DM, Huisman HJ, van Oort IM, Witjes JA, Hulsbergen-van de Kaa CA, et al. Relationship between apparent diffusion coefficients at 3.0-T MR imaging and Gleason grade in peripheral zone prostate cancer. *Radiology* 2011;259:453-461
28. Vos EK, Litjens GJ, Kobus T, Hambrock T, Hulsbergen-van de Kaa CA, Barentsz JO, et al. Assessment of prostate cancer aggressiveness using dynamic contrast-enhanced magnetic resonance imaging at 3 T. *Eur Urol* 2013;64:448-455
29. Oto A, Yang C, Kayhan A, Tretiakova M, Antic T, Schmid-Tannwald C, et al. Diffusion-weighted and dynamic contrast-enhanced MRI of prostate cancer: correlation of quantitative MR parameters with Gleason score and tumor angiogenesis. *AJR Am J Roentgenol* 2011;197:1382-1390
30. Bae H, Yoshida S, Matsuoka Y, Nakajima H, Ito E, Tanaka H, et al. Apparent diffusion coefficient value as a biomarker reflecting morphological and biological features of prostate cancer. *Int Urol Nephrol* 2014;46:555-561
31. Nagel KN, Schouten MG, Hambrock T, Litjens GJ, Hoeks CM, ten Haken B, et al. Differentiation of prostatitis and prostate cancer by using diffusion-weighted MR imaging and MR-guided biopsy at 3 T. *Radiology* 2013;267:164-172
32. Zakian KL, Sircar K, Hricak H, Chen HN, Shukla-Dave A, Eberhardt S, et al. Correlation of proton MR spectroscopic imaging with gleason score based on step-section pathologic analysis after radical prostatectomy. *Radiology* 2005;234:804-814
33. Wang L, Mazaheri Y, Zhang J, Ishill NM, Kuroiwa K, Hricak H. Assessment of biologic aggressiveness of prostate cancer: correlation of MR signal intensity with Gleason grade after radical prostatectomy. *Radiology* 2008;246:168-176
34. Lemaitre L, Puech P, Poncelet E, Bouyé S, Leroy X, Biserte J, et al. Dynamic contrast-enhanced MRI of anterior prostate cancer: morphometric assessment and correlation with radical prostatectomy findings. *Eur Radiol* 2009;19:470-480
35. Bratan F, Melodelima C, Souchon R, Hoang Dinh A, Mège-Lechevallier F, Crouzet S, et al. How accurate is multiparametric MR imaging in evaluation of prostate cancer

volume? *Radiology* 2015;275:144-154
36. Lencioni R, Menchi I, Paolicchi A, Carini M, Amorosi A, Bartolozzi C. Prediction of pathological tumor volume in clinically localized prostate cancer: value of endorectal coil magnetic resonance imaging. *MAGMA* 1997;5:117-121
37. Coakley FV, Kurhanewicz J, Lu Y, Jones KD, Swanson MG, Chang SD, et al. Prostate cancer tumor volume: measurement with endorectal MR and MR spectroscopic imaging. *Radiology* 2002;223:91-97
38. Le Nobin J, Orczyk C, Deng FM, Melamed J, Rusinek H, Taneja SS, et al. Prostate tumour volumes: evaluation of the agreement between magnetic resonance imaging and histology using novel co-registration software. *BJU Int* 2014;114(6b):E105-E112
39. Anwar M, Westphalen AC, Jung AJ, Noworolski SM, Simko JP, Kurhanewicz J, et al. Role of endorectal MR imaging and MR spectroscopic imaging in defining treatable intraprostatic tumor foci in prostate cancer: quantitative analysis of imaging contour compared to whole-mount histopathology. *Radiother Oncol* 2014;110:303-308
40. Ouzzane A, Helfrich O, Le Nobin J, Puech P, Betrouni N, Villers A. Understanding the pathological implications of MRI: application to focal therapy planning. *Curr Opin Urol* 2015;25:198-204
41. Fütterer JJ. MR imaging in local staging of prostate cancer. *Eur J Radiol* 2007;63:328-334
42. Fütterer JJ, Engelbrecht MR, Huisman HJ, Jager GJ, Hulsbergen-van De Kaa CA, Witjes JA, et al. Staging prostate cancer with dynamic contrast-enhanced endorectal MR imaging prior to radical prostatectomy: experienced versus less experienced readers. *Radiology* 2005;237:541-549
43. Vargas HA, Hötker AM, Goldman DA, Moskowitz CS, Gondo T, Matsumoto K, et al. Updated prostate imaging reporting and data system (PIRADS v2) recommendations for the detection of clinically significant prostate cancer using multiparametric MRI: critical evaluation using whole-mount pathology as standard of reference. *Eur Radiol* 2016;26:1606-1612
44. Lim CS, McInnes MD, Lim RS, Breau RH, Flood TA, Krishna S, et al. Prognostic value of Prostate Imaging and Data Reporting System (PI-RADS) v. 2 assessment categories 4 and 5 compared to histopathological outcomes after radical prostatectomy. *J Magn Reson Imaging* 2016 Nov 3 [Epub ahead of print]. http://dx.doi.org/10.1002/jmri.25539
45. Rosenkrantz AB, Ginocchio LA, Cornfeld D, Froemming AT, Gupta RT, Turkbey B, et al. Interobserver reproducibility of the PI-RADS version 2 lexicon: a multicenter study of six experienced prostate radiologists. *Radiology* 2016;280:793-804
46. Schoots IG, Roobol MJ, Nieboer D, Bangma CH, Steyerberg EW, Hunink MG. Magnetic resonance imaging-targeted biopsy may enhance the diagnostic accuracy of significant prostate cancer detection compared to standard transrectal ultrasound-guided biopsy: a systematic review and meta-analysis. *Eur Urol* 2015;68:438-450
47. de Rooij M, Hamoen EH, Fütterer JJ, Barentsz JO, Rovers MM. Accuracy of multiparametric MRI for prostate cancer detection: a meta-analysis. *AJR Am J Roentgenol* 2014;202:343-351
48. Sharif-Afshar AR, Nguyen C, Feng TS, Payor L, Fan Z, Saouaf R, et al. Prospective pilot trial to evaluate a high resolution diffusion-weighted MRI in prostate cancer patients. *EBioMedicine* 2016;7:80-84
49. Barentsz JO, Weinreb JC, Verma S, Thoeny HC, Tempany CM, Shtern F, et al. Synopsis of the PI-RADS v2 guidelines for multiparametric prostate magnetic resonance imaging and recommendations for use. *Eur Urol* 2016;69:41-49